Pedogenic calcite as evidence for an early Holocene dry period in the San Francisco Bay area, California

Glenn Borchardt* *Soil Tectonics, P.O. Box 5335, Berkeley, California 94705* and *California Department of Conservation, Division of Mines and Geology, Suite 210, San Francisco, California 94107*

James J. Lienkaemper *U.S. Geological Survey, 345 Middlefield Road, Menlo Park, California 94025*

ABSTRACT

Rainfall at the site of Union City, California, during early Holocene time appears to have been about half that of today, 470 mm/yr. We base this conclusion on detailed descriptions and particle-size analyses of 12 soil profiles and 1:20 scale logs of the fluvial stratigraphy in two 100-m-long, 5-m-deep excavations dug perpendicular to the axis of an alluvial fan along the Hayward fault. Subsidence and right-lateral movement along the fault allowed an offset stream to produce a nearly continuous alluvial record documented by 35 ^{14}C ages on detrital charcoal. Bk (calcitic) horizons in paleosols developed in the fan suggest that a relatively dry climatic period occurred from 10 to 7 ka (calendar-corrected ages). The pedogenic calcite exists primarily as vertically oriented filaments and fine, cavernous nodules formed at ped intersections. Soils and paleosols formed before 10 ka or since 7 ka did not have Bk horizons. Bk horizons that were buried suddenly at 7 ka were overlain by leached zones averaging 41 ± 3 cm thick—about half the current depth of leaching.

INTRODUCTION

Calcite precipitates in soils when Ca^{2+} from rainwater or soil minerals comes in contact with dissolved CO_3^{2-} from rainwater, root respiration, plant decomposition, or soil minerals. Arid and semiarid climates are ideal for pedogenic calcite formation because short periods of precipitation foster the dissolving stage, whereas long periods of evapotranspiration foster the concentrating stage. Calcareous soil horizons generally are overlain by a leached horizon, the thickness of which is related to mean annual precipitation, as modified by soil texture, porosity, pore-size distribution, vegetative cover, slope, aspect, seasonality, and other factors (Arkley, 1963; McFadden and Tinsley, 1985; McFadden et al., 1991). At this latitude, when mean annual precipitation is much greater than 500 mm/yr, pedogenic calcite generally does not form in soils developed on noncalcareous parent materials (Birkeland, 1984).

The properties of calcareous soils can reveal that the climate is now drier than it was in the past (Birkeland, 1984). In the Mojave Desert, for example, Holocene Bk horizons are shallow and have weak development, while the underlying Pleistocene Bk and K horizons are three times as deep and have strong development (McFadden and Tinsley, 1985). In Holocene soils it is difficult, however, to show that the climate is now wetter than it was in the past. This is because an increase in precipitation causes delicate forms of calcite (stage I, Gile et al., 1966) to be dissolved and removed from the soil profile. However, as we show here, suitably aggrading environments can protect calcareous paleosols, preserving a record of a climate that was drier than at present. In this paper we use ^{14}C dates on associated charcoal samples to show that the Union City, California, area probably had half the present rainfall in early Holocene time, between 10 and 7 ka (calendar corrected ages designated according to international convention reiterated by Colman et al., 1987).

STUDY SITE

At Union City, California, Masonic Creek cuts through the East Bay Hills on the northeast side of the Hayward fault and debouches onto a well-drained alluvial fan on the southwest (Figs. 1 and 2). The fan sediments were derived mostly from the Orinda Formation, a Pliocene continental

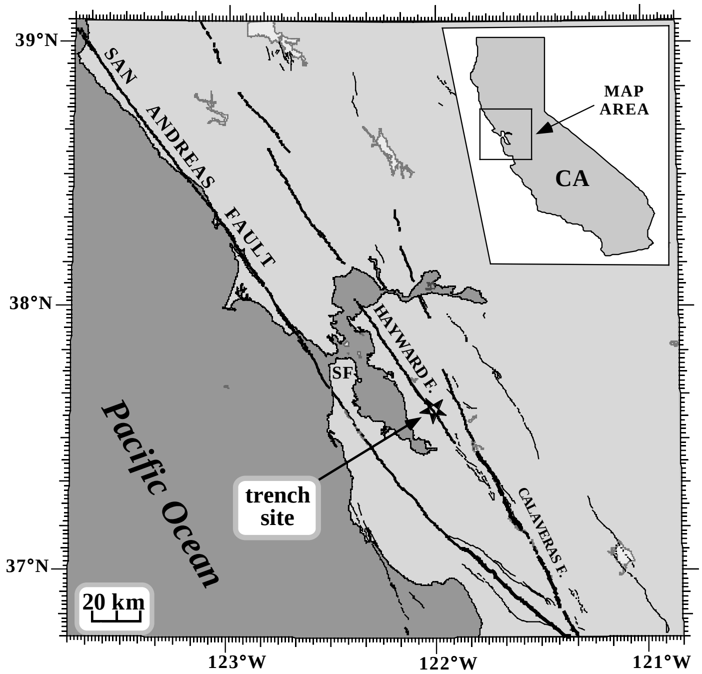

Figure 1. Location of the trench site along the Hayward fault (F.), Union City, California (from Lienkaemper and Borchardt, 1996).

*E-mail: gborchardt@usa.net.

GSA Bulletin; June 1999; v. 111; no. 6; p. 906-918; 7 figures; 6 tables.

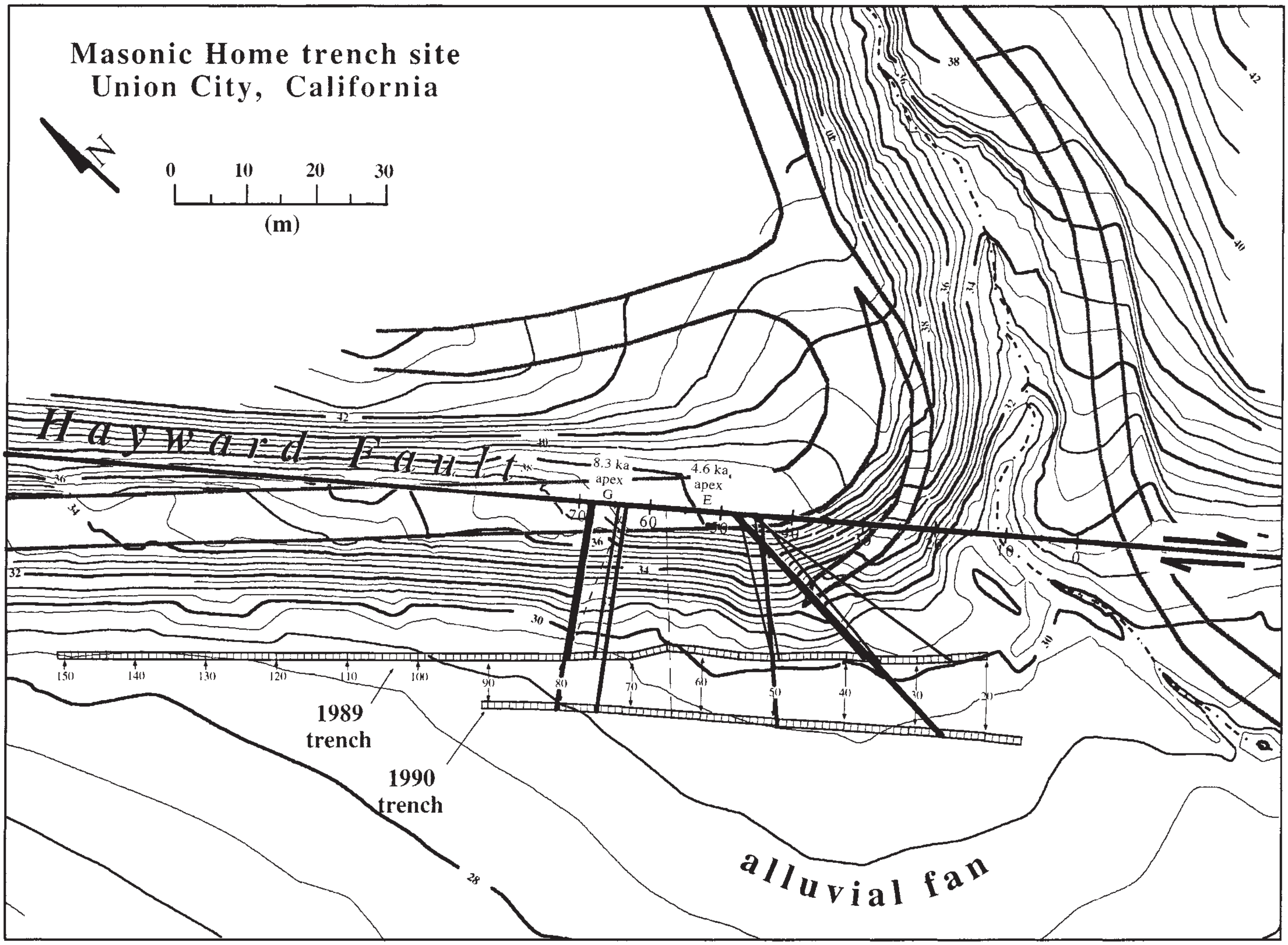

Figure 2. Site map modified from Lienkaemper and Borchardt (1996) showing trench excavations across the alluvial fan on the southwest side of the Hayward fault (heavy horizontal line). Masonic Creek (dashed line) approaches from the northeast, crosses the fault, and continues southward along the southeastern flank of the modern fan surface. Paleochannels (thick solid lines projected from the trenches to the fault plane) that were evident in the trench stratigraphy were oriented toward either of two fan apexes. Rapid aggradation at 7 ka preserved the pedogenic calcite associated with the buried fan surface that debouched at apex G, which is now tectonically offset 66 m from its original position. Contours in 0.5 m intervals are based on a topographic map prepared by using a total station instrument. Solid lines crosscutting the contours on either side of the creek represent streets.

deposit that contributed clay to overbank deposits and gravel to channel deposits. The Miocene Monterey Formation contributed a few angular clasts derived from marine shale and chert from an outcrop 0.5 km upstream.

The watershed of Masonic Creek is 1.3 km^2, with slopes of about 25% that are subject to the development of cohesive, rotational landslides. Debris flows apparently do not form in the watershed. Even though the overbank deposits were mostly clayey, no perched water conditions were evident in the fan. The climate is Mediterranean with seasonal rainfall increasing from 470 mm/yr on the fan at the 30 m elevation to 635 mm/yr on the ridge crest at the 293 m elevation (Rantz, 1971).

We described and sampled soil profiles at 10 m intervals in a 130-m-long, 5-m-deep trench excavated parallel to the Hayward fault and perpendicular to the axis of this fan (Fig. 3). Along with a detailed log of the trench walls, these soil profiles enabled us to study a series of channel fills and interfingered and interleaved paleosols that form a complex of buried alluvial fans. We found that the Hayward fault had been moving right laterally at this location at about 8 ± 1 mm/yr during Holocene time (Lienkaemper and Borchardt, 1996). Thus, the fan apex initiated at 8.3 ka was offset 66 m and the one initiated at 4.6 ka was offset 42 m (Fig. 2). The southwest side of the fault subsides at 0.6 ± 0.1 mm/yr, thus providing the opportunity for multiple buried paleosols to be preserved within the fan complex.

METHODS

The trenches were logged in detail at a scale of 1:20. The logs are archived at the U.S. Geological Survey, the geologic detail having been reduced and interpreted for this study. The soil stratigraphic results and interpretations are abstracted on a horizontally reversed image of the northeast

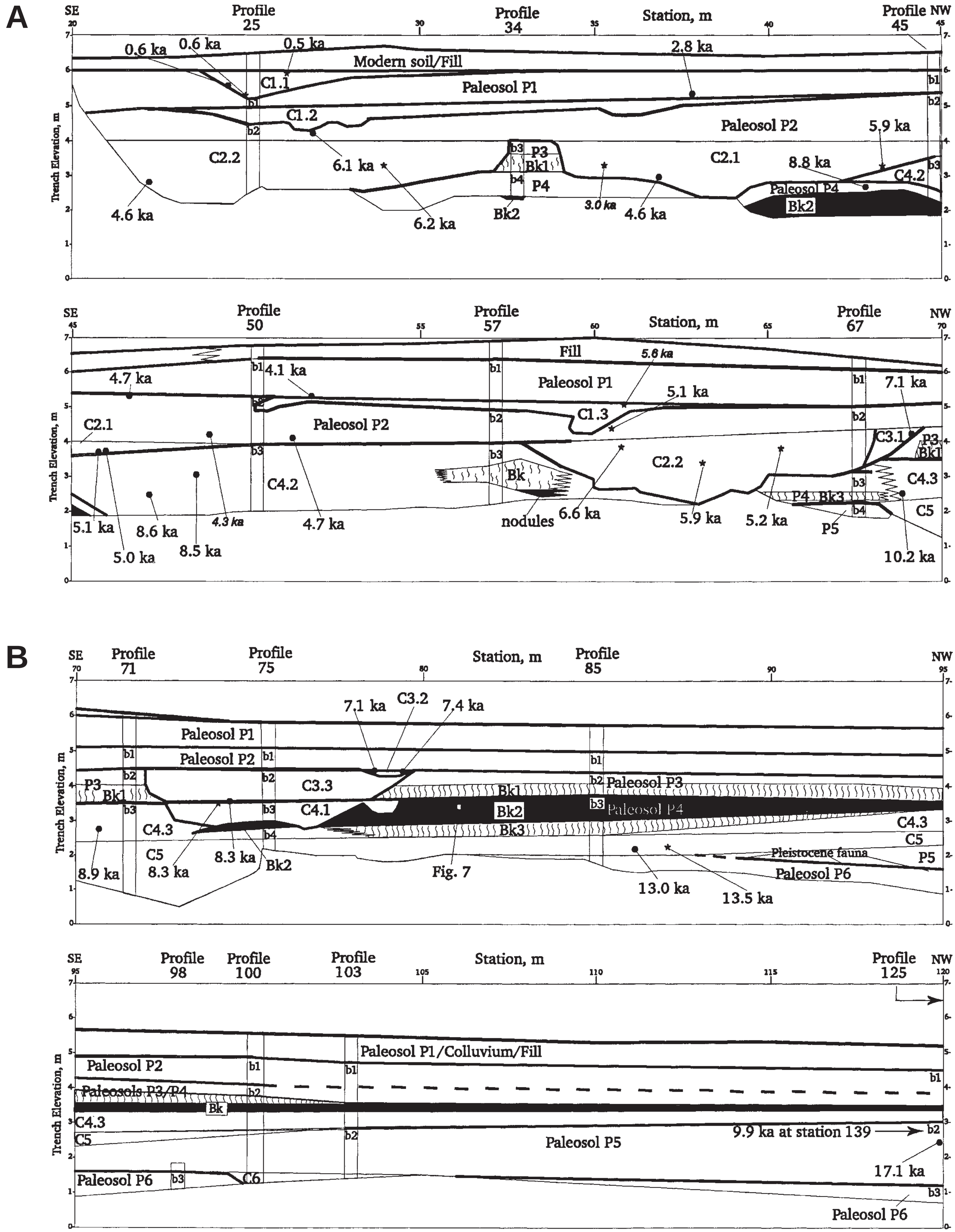
A
SE
Profile 25
Profile 34
Station, m
Profile 45
NW
Trench Elevation, m
0.6 ka
0.6 ka
0.5 ka
2.8 ka
Modern soil/Fill
C1.1
Paleosol P1
C1.2
Paleosol P2
5.9 ka
C2.2
6.1 ka
P3
Bk1
C2.1
8.8 ka
C4.2
P4
Paleosol P4
Bk2
4.6 ka
6.2 ka
Bk2
3.0 ka
4.6 ka
SE
Profile 50
Profile 57
Station, m
Profile 67
NW
Fill
5.6 ka
4.7 ka
4.1 ka
Paleosol P1
7.1 ka
5.1 ka
C1.3
C2.1
Paleosol P2
C3.1
P3
Bk1
C2.2
Bk
C4.3
C4.2
P4
Bk3
C5
P5
5.1 ka
8.6 ka
4.3 ka
4.7 ka
nodules
6.6 ka
5.9 ka
5.2 ka
5.0 ka
8.5 ka
10.2 ka
B
SE
Profile 71
Profile 75
Station, m
Profile 85
NW
7.1 ka
C3.2
7.4 ka
Paleosol P1
Paleosol P2
C3.3
Paleosol P3
P3
Bk1
Bk1
C4.1
Bk2
Paleosol P4
C4.3
Bk3
C4.3
C5
C5
Pleistocene fauna
P5
8.9 ka
8.3 ka
8.3 ka
Bk2
Fig. 7
Paleosol P6
13.0 ka
13.5 ka
SE
Profile 98
Profile 100
Profile 103
Station, m
Profile 125
NW
Paleosol P1/Colluvium/Fill
Paleosol P2
Paleosols P3/P4
Bk
C4.3
C5
9.9 ka at station 139
Paleosol P5
17.1 ka
Paleosol P6
C6
Paleosol P6

wall of the 130 m trench at a scale of 1:100 (Fig. 3). This figure also includes important charcoal ages (Table 1) from other exposures. Except for one sample, accelerator mass spectroscopy (AMS) dating determined the ages of the detrital charcoal samples. More than 200 charcoal specimens were collected, the criteria for analysis favoring strategic locations in horizontally continuous units without krotovinas (soil-filled burrows). Where possible, the least abraded, most rectangular samples having distinct plant structure were selected for analysis. The presence of a few discordant dates (Fig. 3) shows that the criteria were not always met. Nevertheless, we were able to obtain sufficient replication to date the depositional sequence for the 4.6 ka and 8.3 ka fans within a standard deviation of 50 yr (Lienkaemper and Borchardt, 1996). In general, we considered the youngest charcoal within a channel fill to be the best representation of its burial age. Thus, channel C3.2 at station 79 (Fig. 3B), for example, had detrital charcoal samples dated as 7.1 ± 0.1 ka and 7.4 ± 0.1 ka. The 7.4 ka charcoal could be from heartwood of a centuries-old tree or could have lain in the watershed for several centuries before being deposited in the channel. We consider these possibilities to be greater than any due to analytical error or contamination.

Station and soil profile numbers refer to the distance northwest from the current active channel of the contributing stream, informally known as Masonic Creek. The soil profiles were sampled and described by the standard methods outlined by the Soil Survey Staff (1951, 1975). In these descriptions the first buried soil encountered at a particular station is labeled b1. Still deeper buried soil surfaces are labeled b2, b3, and so on. The Bt and Bk designations are not diagnostic. They are used simply to indicate the presence of clay films and calcite. The P designations (e.g., Paleosol P3, Fig. 3) represent cross-correlated surfaces derived from all profile descriptions and trench logs. The C designations (e.g., C3, Fig. 3) are sands and gravels generally composed of numerous inset channel fills that were active when the paleosol with the same numerical designation composed the surface of the remainder of the fan. Toward the end of a channel's life, it typically becomes buried by fine materials that we consider to be essentially the same age. Thus, the channel associated with a particular surface may have deposited overbank materials that were later cut by that same channel. The profile showing the best development of the youngest four paleosols is described in Table 2; the other profiles were described in Borchardt (1992a). The particle-size analyses (Table 3) were done by using the standard American Society for Testing and Materials (ASTM) hydrometer and sieve methods. The pedochronology (Borchardt, 1992b) was developed as described in Borchardt (1992a). In essence, pedochronology is the study of pedogenesis with regard to the determination of when soil formation began, how long it occurred (with or without aggradation), and when it stopped. The study of paleosols, in particular, requires knowledge of two ages and the calculated duration: t_o, age when soil formation and/or aggradation began (ka); t_b, age when soil or strata was buried (ka); and t_d, duration of soil development and/or aggradation (k.y.)

Figure 3. (A) Simplified, reversed, and reduced-scale log of the soil and alluvial relationships parallel and southwest of the Hayward fault at Union City. The 1989 trench was used as the base. This interpretation emphasizes paleosurfaces indicated in each soil profile by lowercase letters followed by sequence numerals (e.g., b1, b2). Cross-correlated surfaces appear as paleosols P1 through P6. Their contemporaneous channel cuts and generally nested fills in these surfaces are indicated with associated letters and numbers indicating increasing age (e.g., C1, C2). Thick lines are actual contacts, and thin lines are projections of former surfaces. Dashed lines are conjectural. Feathered contacts are particularly diffuse due to textural gradations. Abbreviations: ka—^{14}C date corrected to thousands of calendar years; Bk—soil horizon containing calcite (dark shading—nodules; light shading—filaments); asterisk—charcoal from this exposure; filled circle—charcoal location interpreted from an adjacent exposure; diminutive italics indicate discordant ages. Stations 20 to 70. (B) Stations 70 to 120.

RESULTS

Fan Evolution

During Pleistocene time, the Masonic Creek fan had thin, distributary channel fills showing minimal aggradation (e.g., C5, Fig. 3b). During the Holocene, the fan had thick, relatively confined channel fills with pronounced aggradation (e.g., C2, Figs. 3A and 4). The most significant Holocene degradation occurred when new apexes were formed at 8.3 ka and 4.6 ka (Figs. 2 and 4). The locations of these apexes were determined in an earlier study that used channel width and thickness, cobble size, base level, age, and relation to paleosols to correlate the major channels in the two trenches, which were excavated parallel to the Hayward fault (Fig. 2; Lienkaemper and Borchardt, 1996). The locations of correlative channels in the two trenches were used to project lines toward the fault plane, thus delineating the locations of the apexes used to determine fault offset.

Holocene degradation occurred primarily near the axis of the fan, and aggradation occurred away from it. Thus only aggradation occurred northwest of station 80 during the past 10 k.y. (Fig. 3B), while both degradation and aggradation occurred to the southeast. Aggradation at station 85 seems to have been relatively continuous both before and after 8.3 ka, when apex G was formed. For the inception of apex G to have occurred, however, the channel would have had to be filling before 8.3 ka. After 8.3 ka the channel would have been cutting. This is because the stream gradient would have been increased when the low-gradient offset in the stream was abandoned for a shorter path. Nevertheless, except for a slight coarsening (Fig. 5) due to increased source distance, the deposition of clayey overbank materials continued unabated at station 85. Thus, we conclude that Holocene overbank aggradation occurred sporadically on the fan despite occasional degradation in the channel.

Soil Stratigraphy

The complex stratigraphy of the Masonic Creek alluvial fan includes a modern soil and six major paleosols formed since 24 ka, as summarized in Table 4 and Fig. 6. For thin alluvial units such as these, the resulting pedochronology necessarily must be idealized. The burial of a soil by a thin alluvial unit often changes, but does not preclude the continuing development of that buried soil. Thus, the t_d of the modern soil is an absolute duration (0.5 k.y.), while the t_d of the underlying paleosol is a minimum (4.1 ka, Fig. 6). For the most part, the paleosols are developed in clayey overbank deposits (Table 3), the episodic accumulation of which was typically contemporaneous with soil development. The locations and primary characteristics of the best-developed sections are as follows.

Modern Soil. This black soil, as much as 60 cm thick, overlies the gravels and sands of the youngest channel in the trench (Fig. 3A, station 25; Table 3, soil profile 25; Fig. 6). It has been the surface soil between station 0 and station 50 since 0.5 ka, when the finely bedded strata at the top of channel C1.1 was suddenly buried. It has coarse moderate granular structure.

Paleosol P1. This paleosol has a black, 60-cm-thick A horizon overlying a very dark brown, 30-cm-thick B horizon that has fine moderate prismatic structure (Table 3, soil profile 67). Paleosol P1 formed in an overbank unit, the thickness of which gradually decreased from 120 cm at station 20 to

TABLE 1. AGES OF CHARCOAL SAMPLES FROM THE TRENCH SITE

Elevation (m)*	Station (m)	Field number	Trench wall	Laboratory number	^{14}C yr B.P.	ka†	Associated paleosol
6.1	26.7	89B341	NE	AA-4657	415 ± 60	0.49 ± 0.07	Modern
5.5	22.8	89B134	SW	I-15,819	510 ± 80	0.58 ± 0.07	Modern
5.4	24.6	89B142	NE	AA-4649	580 ± 70	0.63 ± 0.05	Modern
5.3	37.6	89B162	SW	AA-8906	2665 ± 60	2.82 ± 0.06	P1§
3.3	35.3	89B201	NE	AA-8907	2845 ± 50	3.02 ± 0.08	P2
3.8	49.7	90B161	SW	AA-6814	3700 ± 60	4.10 ± 0.09	P1
3.8	49.1	89B271	SW	AA-4653	3800 ± 100	4.25 ± 0.14	P2
1.7	16.2	90B314	SW	AA-6824	4000 ± 70	4.56 ± 0.13	P2
3.0	37.1	89B175	SW	AA-4651	4065 ± 100	4.64 ± 0.14	P2
3.9	47.6	90B158	SW	AA-6816	4145 ± 55	4.73 ± 0.10	P1/P2
3.2	51.3	90B166	SW	AA-6817	4160 ± 60	4.73 ± 0.09	P2
3.0	46.3	90B144	SW	AA-8912	4320 ± 50	4.95 ± 0.06	P2
4.2	60.4	89B300	NE	AA-8909	4395 ± 60	5.05 ± 0.11	P2
3.0	45.7	90B142	SW	AA-6822	4430 ± 60	5.10 ± 0.12	P
3.8	65.3	89B274	NE	AA-8908	4520 ± 50	5.21 ± 0.08	P2
5.1	60.8	89B292	NE	AA-4654	4805 ± 60	5.59 ± 0.08	P1
3.5	63.5	89B312	NE	AA-8910	5135 ± 60	5.91 ± 0.07	P2
2.6	42.6	90B108	SW	AA-8911	5145 ± 70	5.94 ± 0.09	P2
3.2	25.8	90B283	SW	AA-6813	5240 ± 60	6.08 ± 0.08	P2
3.2	29.1	89B139	NE	AA-4648	5400 ± 100	6.22 ± 0.12	P2
3.8	61.0	89B298	NE	AA-4655	5750 ± 100	6.62 ± 0.11	P
3.9	80.2	90B262	SW	AA-6820	6110 ± 60	7.06 ± 0.09	P2/P3
3.5	62.5	90B212	SW	AA-9603	6145 ± 70	7.08 ± 0.08	P3
4.2	79.6	89L013	SW	AA-4660	6470 ± 120	7.39 ± 0.10	P2/P3
3.3	74.0	89B031	SW	AA-4259	7435 ± 60	8.27 ± 0.08	P3/P
2.8	74.7	90B222	SW	AA-6815	7430 ± 70	8.27 ± 0.09	P3/P4
2.1	36.4	90B090	SW	AA-6818	7680 ± 70	8.51 ± 0.08	P4
2.5	46.6	89B191	SW	AA-4652	7740 ± 110	8.60 ± 0.16	P4
2.3	40.9	90B105	SW	AA-6823	7890 ± 100	8.78 ± 0.15	P4
2.5	69.7	89B349	SW	AA-4658	8055 ± 130	8.92 ± 0.16#	P4
3.1	138.6	89B099	SW	AA-4646	8740 ± 90	9.93 ± 0.10#	P5
2.2	64.9	90B214	SW	AA-6819	9260 ± 70	10.24 ± 0.08#	P4
1.5	85.5	90B249	SW	AA-6821	11010 ± 80	12.97 ± 0.09#	P5
2.4	87.0	89L033	NE	AA-4663	11560 ± 100	13.52 ± 0.14#	P5
2.5	121.5	89L021	SW	AA-4662	14200 ± 160	17.08 ± 0.19#	P5

Note: Data partially from Lienkaemper and Borchardt (1996). AA—Laboratory determination by National Science Foundation, National Accelerator Facility for Radioisotope Analyses, Department of Physics, PAS 81, University of Arizona, Tucson, Arizona 85721. I—Laboratory determination by Teledyne Isotopes, Inc., 50 Van Buren Ave., Westwood, New Jersey 07675. Standard deviation includes only analytical error. Uncorrected ^{14}C dates expressed in yr B.P. (^{14}C years before 1950).

*Elevation from base of trench.

†Calibrated ages expressed in ka (thousands of calendar years before 1990) and calculated by using program Calib ETH 1.5b (ETH Zurich of 1991) and ATM20.C14B calibration file (Linick et al., 1986). Sample 90B214 was calibrated by using file Stuiver3.C14B (Stuiver et al., 1991). Samples 90B249 and 89L033 were calibrated by using the program of Stuiver and Reimer (1993), revision 3.0.3c.

§P1 = first major paleosol, and so on.

#Calibrated with the equation: calendar yr = 1.3111(^{14}C yr)–1533 yr, developed from Bard et al. (1990) and Borchardt and Seelig (1991), who correct 21 000 yr B.P. to 26 ka by using ^{230}Th/^{234}U analyses on coral and cacite concretions, respectively.

60 cm at station 100. The Bt horizon has a few thin clay films on clasts, pores, and ped faces. The beginning of the deposition associated with P1 coincided with the inception of fan apex E (Lienkaemper and Borchardt, 1996; Fig. 2). The channel fills associated with the deposition and dissection of this overbank parent material become progressively younger to the southeast, where we found charcoal as young as 2.8 ka (Fig. 3A). Thus, most of paleosol P1 is younger than the best-developed section represented by soil profile 67.

Paleosol P2. This paleosol has a very dark brown Bt horizon as much as 70 cm thick overlying an 80-cm-thick dark brown BCt horizon (Table 3, soil profile 67; Fig. 6). Initially, the A horizon of paleosol P2 became the B horizon of paleosol P1. The structure of paleosol P2 ranges from fine, moderate, angular blocky to massive. It once was the surface soil between station 0 and station 130. Except for the overlying fill and the colluvium eroded from the fault scarp, it would remain today as the surface soil between station 100 and station 130. It has common to many thin clay films on clasts in the Bt horizon and many moderately thick clay films lining pores in the BCt horizon. The channel fills associated with the deposition of this overbank material become progressively younger to the southeast, where we found charcoal as young as 4.6 ka (Fig. 3A, station 37). Overbank deposition associated with P2 northwest of station 67 occurred immediately after 7.1 ka, when the thinly bedded sediments at the top of channel C3.2 were suddenly buried (Fig. 3B, station 79). Farther to the southeast, the overbank deposition associated with P2 was considerably younger.

Paleosol P3. This paleosol has a 45-cm-thick, dark grayish-brown Bt horizon overlying a 30-cm-thick, very dark grayish-brown BCtk horizon (Table 3, soil profile 85; Fig. 6). The structure ranges from medium to coarse, strong, angular blocky. There are a few thin patchy clay films and mangans on clasts in the Bt horizon. These probably formed in a former A horizon during its postburial pedogenesis as a B horizon. The contact between paleosols P2 and P3 between stations 80 and 100 shows no signs of erosion sufficient to have removed the A horizon from paleosol P3 (Fig. 3B). The BCtk (denoted Bk1 in Fig. 3) has a pH of 8.1 and contains thin vertically oriented calcite filaments along ped faces. The beginning of the deposition associated with paleosol P3 coincided with the inception of fan apex G (Fig. 2). The 8.3 ka age was obtained from duplicate samples

TABLE 2. COMPLETE DESCRIPTION OF SOIL PROFILE 85

Horizon	Depth (cm)	Trench elevation (m)	Description
A	0–30	5.66–5.36	PALEOSOL P1 (RELICT): Very dark gray (10YR3/1m, 4/1d) clay loam; medium moderate subangular to angular blocky structure; sticky and plastic when wet, friable when moist, and very hard when dry; very few, very fine roots; common very fine discontinuous and continuous random tubular pores; rare reworked peds with few thin patchy high chroma clay films; gradual smooth boundary; pH 7.2; conductivity 580 uS (Sample 89B032).
AB	30–63	5.36–5.03	Black (10YR2/1m, 4/1d) clay loam; medium moderate strong angular blocky to prismatic structure; sticky and plastic when wet, firm when moist, and very hard when dry; few very fine continuous random tubular pores; rare reworked peds with few thin patchy high chroma clay films; diffuse smooth boundary; pH 7.3; conductivity 700 uS (Sample 89B033). PALEOSOL P1.
PEDOCHRONOLOGY:		t_o = **4.6 ka** t_b = **0 ka** t_d = **4.6 k.y.**	
AB1b1	63–100	5.03–4.66	PALEOSOL P2: Black (10YR2/1m, 4/1d) clay loam; medium moderate strong angular blocky to prismatic structure; sticky and very plastic when wet, friable when moist, and very hard when dry; few very fine continuous random tubular pores; rare reworked peds with few thin patchy high chroma clay films; clear smooth boundary; pH 7.5; conductivity 730 uS (Sample 89B034).
AB2b1	100–120	4.66–4.46	Very dark grayish brown (10YR3/2m, 4/2d) clay loam; medium strong angular blocky structure; sticky and very plastic when wet, friable when moist, and very hard when dry; few very fine continuous random tubular pores; few thin patchy clay films on sand grains, clasts, and ped faces; clear smooth boundary; pH 7.7; conductivity 740 uS (Sample 89B035). PALEOSOL P2.
PEDOCHRONOLOGY:		t_o = **7.1 ka** t_b = **4.6 ka** t_d = **2.5 k.y.**	
2Btb2	120–166	4.46–4.00	PALEOSOL P3: Dark grayish brown (10YR4/2m, 5/2d) clay; medium angular blocky structure; sticky and very plastic when wet, friable when moist, and very hard when dry; few very fine continuous random tubular pores; few thin patchy clay films on sand grains, clasts, and ped faces; few manganese oxide coatings lining pores; gradual smooth boundary; pH 8.0; conductivity 800 uS (Sample 89B036).
2BCtkb2	166–195	4.00–3.71	Very dark grayish brown (10YR3/2m, 4/2d) clay with common fine to medium prominent white (10YR8/2md) mottles; coarse strong angular blocky structure; sticky and very plastic when wet, friable when moist, and very hard when dry; few very fine roots in pores lined with calcite; few very fine continuous random tubular pores; few thin patchy clay films on sand grains, clasts, and ped faces; few mostly vertically oriented calcite filaments with violent effervescence; abrupt smooth boundary; pH 8.1; conductivity 790 uS; denoted as Bk1 in Fig. 3 (Sample 89B037).
PEDOCHRONOLOGY:		t_o = **8.3 ka** t_b = **7.1 ka** t_d = **1.2 k.y.**	
2Atkb3	195–215	3.71–3.51	PALEOSOL P4: Very dark grayish brown (10YR3/2m, 5/2d) clay with few fine prominent white (10YR8/2md) mottles; medium to coarse strong angular blocky structure; sticky and very plastic when wet, firm when moist, and very hard when dry; few very fine roots in pores lined with calcite; few very fine continuous random tubular pores; few thin patchy clay films coating clasts; few mostly vertically oriented calcite filaments and fine nodules with violent effervescence; many pressure faces; gradual smooth boundary; pH 8.2; conductivity 960 uS; denoted as Bk2 in Fig. 3 (Sample 89B038).
2Btkb3	215–265	3.51–3.01	Dark grayish brown (10YR4/2m, 5/2d) clay with common fine to medium prominent white (10YR8/2md) mottles; medium to coarse strong angular blocky to prismatic structure; sticky and very plastic when wet, firm when moist, and very hard when dry; few very fine continuous random tubular pores; few thin patchy clay films coating clasts; common fine calcite nodules at ped intersections coated with calcite filaments; violent effervescence; many pressure faces; clear smooth boundary; pH 8.2; conductivity 930 uS; denoted as Bk2 in Fig. 3 (Sample 89B039).
3BC1tkb3	265–286	3.01–2.80	Brown (10YR4/3m, 6/3d) clay loam with common fine to medium prominent white (10YR8/2md) mottles; medium weak subangular blocky to massive structure; sticky and plastic when wet, friable when moist, and very hard when dry; few very fine continuous random tubular pores; few thin clay films on coating calcite lining pores; common calcite filaments; disseminated charcoal; clear smooth boundary; pH 8.4; conductivity 640 uS; denoted as Bk3 in Fig. 3 (Sample 89B040).
3BC2tkb3	286–307	2.80–2.59	Brown (10YR4/3m, 6/3d) clay loam with few fine prominent white (10YR8/2md) mottles; medium weak subangular blocky to massive structure; sticky and slightly plastic when wet, very friable when moist, and very hard when dry; few very fine continuous random tubular pores; few thin to medium thick clay films lining pores and few thin patchy clay films coating clasts; rare calcite filaments; disseminated charcoal; clear smooth boundary; pH 7.8; conductivity 510 uS; denoted as Bk3 in Fig. 3 (Sample 89B041).
3BCtb3	307–329	2.59–2.37	Brown (10YR5/3m, 6/3d) sandy clay loam; medium weak subangular blocky to massive structure; sticky and slightly plastic when wet, very friable when moist, and very hard when dry; few very fine continuous random tubular pores; few thin to medium thick clay films lining pores and few thin patchy clay films coating clasts to 50 cm; clear smooth boundary; pH 7.9; conductivity 420 uS (Sample 89B042) (Sample 89B047 was taken of the entire Bk horizon from 120–329 cm).
4BCtb3	329–341	2.37–2.25	Dark yellowish–brown (10YR4/4m, 6/4d) gravelly sandy clay loam; medium weak subangular blocky to massive structure; sticky and slightly plastic when wet, very friable when moist, and very hard when dry; few very fine continuous random tubular pores; common medium thick clay films lining pores and many thick clay films coating clasts; clear smooth boundary; pH 8.0; conductivity 350 uS (Sample 89B043).
5BCtb3	341–353	2.25–2.13	Brown (10YR4/3m, 6/4d) clay loam; medium weak subangular blocky to massive structure; sticky and slightly plastic when wet, very friable when moist, and very hard when dry; few very fine continuous random tubular pores; common medium thick clay films lining pores and many thick clay films coating clasts; abrupt smooth boundary; pH 7.8; conductivity 450 uS (Sample 89B044).
6BCtb3	353–393	2.13–1.73	Brown (10YR4/3m, 6/4d) gravel; massive structure; sticky and slightly plastic when wet, very friable when moist, and very hard when dry; few very fine continuous random interstitial pores; common medium thick clay films lining pores and many thick clay films coating clasts; abrupt smooth boundary; pH 7.8; conductivity 440 uS (Sample 89B045).
7BCtb3	393–410+	1.73–1.56	Dark yellowish brown (10YR4/4m, 6/4d) gravelly clay; medium weak subangular blocky to massive structure; sticky and slightly plastic when wet, very friable when moist, and very hard when dry; few very fine continuous random tubular pores; common medium thick clay films lining pores and many thick clay films coating clasts; pH 7.9; conductivity 530 uS (Sample 89B046).
PEDOCHRONOLOGY:		t_o = 10.0 ka t_b = **8.3 ka** t_d = 1.7 k.y.	

TABLE 3. PARTICLE SIZE DISTRIBUTION OF SELECTED SOIL HORIZONS FROM THE SITE

89B Field number	Trench elevation (m)	Paleosol	Horizon	Total Sand 2.0–0.050	Total Silt 0.05–0.002	Total Clay <0.002	Sand Very Coarse 2–1	Sand Coarse 1–0.5	Sand Medium 0.5–0.25	Sand Fine 0.25–0.10	Sand Very Fine 0.10-0.05	Silt Coarse 0.05–0.02	Silt Medium 0.02–0.005	Silt Fine 0.005–0.002	Gravel of whole sample >20 mm (%)	Texture
				(% of sample <2 mm)												
Soil Profile No. 25																
103	6.14–5.97	M	AB2	39.1	26.2	34.7	5.5	4.8	8.0	12.7	8.0	7.9	11.7	6.7	13.0	cl
105	5.75–4.64	M	3CB	50.0	21.2	28.8	15.1	13.0	8.2	8.8	4.8	5.8	7.9	7.6	67.0	gscl
110	5.19–4.78	P1	8Abb1	36.0	27.2	36.8	2.4	3.3	7.0	14.0	9.3	9.0	12.4	5.8	11.0	cl
117	3.72–2.54	P2	12Btb2	34.3	28.4	37.3	3.3	2.6	6.6	13.1	8.8	9.4	13.0	5.9	12.0	cl
Soil Profile No. 34																
217	4.04–3.66	P3	3Bb3	34.6	28.8	36.6	2.3	2.4	4.8	14.9	10.1	11.2	12.8	4.9	6.0	cl
218	3.66–3.14	P3	3Bkb3	33.6	28.5	37.9	2.1	2.4	4.9	14.8	9.4	9.4	13.4	5.7	13.0	cl
Soil Profile No. 45																
146	6.38–6.00	M	A	34.5	29.4	36.1	2.5	2.9	5.2	13.2	10.7	10.7	13.1	5.6	16.0	gcl
149	5.38–5.07	P2	Ab2	40.3	25.6	34.1	2.4	3.5	8.2	16.9	9.3	7.6	12.1	5.9	15.0	gcl
152	4.58–4.26	P2	2Bt2b2	33.6	28.6	37.8	2.0	1.8	5.9	14.0	9.9	8.9	14.0	5.7	8.0	cl
154	3.48–3.10	P4	2Bt1b3	40.4	27.0	32.6	2.2	2.5	7.6	17.4	10.7	9.0	12.4	5.6	11.0	cl
156	2.20–1.90	P4	3Btkb4	27.6	24.7	47.7	4.1	4.1	4.4	7.1	7.8	10.3	7.0	7.5	13.0	c
Soil Profile No. 50																
221	5.87–5.47	P1	2Btb1	39.3	27.2	33.5	1.2	2.9	7.6	16.4	11.2	10.2	12.4	4.6	3.0	cl
Soil Profile No. 57																
242	5.82–5.27	P1	Btb1	37.2	27.9	34.9	1.2	2.3	6.5	16.7	10.5	9.5	13.7	4.7	14.0	cl
245	4.85–4.24	P2	3Bt1b2	40.6	25.8	33.6	2.3	2.9	7.2	17.7	10.5	9.4	11.9	4.5	3.0	cl
246	4.24–3.91	P2	3Bt2b2	49.1	21.9	29.0	2.1	3.0	10.4	22.8	10.7	8.3	9.0	4.7	2.0	scl
247	3.91–3.28	P3?	3Btb3	38.7	25.2	36.1	3.4	4.0	7.0	16.2	8.1	8.1	11.3	5.8	7.0	cl
248	3.28–2.98	P3?	3Btkb3	31.5	28.3	40.2	0.5	0.5	2.7	14.7	13.2	10.3	11.2	6.7	2.0	c–
249	2.98–2.62	P3?	3BCtkb3	32.6	29.5	37.9	0.6	1.4	4.5	15.2	10.9	10.3	12.6	6.6	1.0	cl
Soil Profile No. 67																
282	4.66–4.15	P2	4Bt1b2	35.4	30.5	34.1	1.0	1.5	6.3	16.5	10.1	10.5	14.7	5.3	1.0	cl
285	3.12–2.56	P4?	4Btb3	36.0	29.9	34.1	1.8	2.1	5.6	16.2	10.4	10.1	15.3	4.4	9.0	cl
286	2.56–2.31	P4?	4Btkb3	30.9	30.9	38.2	1.9	1.5	3.8	13.4	10.3	10.6	15.1	5.2	3.0	cl
Soil Profile No. 71																
317	5.13–4.61	P2	3Btb1	36.0	28.8	35.2	1.0	1.5	5.7	15.9	11.9	9.9	13.8	5.1	3.0	cl
319	4.46–4.08	P3	5Btb2	40.1	27.7	32.2	3.6	3.7	6.1	16.6	10.1	9.0	13.1	5.6	10.0	l
320	4.08–3.79	P3	5Btkb2	36.8	29.5	33.7	1.0	2.1	6.0	14.5	13.2	9.3	15.1	5.1	2.0	l
321	3.79–3.53	P3	5BCtkb2	40.4	29.1	30.5	1.1	1.6	6.8	20.0	10.9	9.6	14.2	5.3	5.0	l
322	3.53–3.22	P4?	5Abtb3	41.8	25.6	32.6	2.3	2.3	7.3	18.9	10.9	9.0	12.0	4.7	14.0	l
Soil Profile No. 75																
49	5.57–5.05	P1	Bt	33.7	22.0	44.3	1.1	1.3	5.3	18.4	7.6	5.7	10.0	6.3	9.0	c
50	5.05–4.72	P2	2Bt1b1	35.8	26.6	37.6	0.8	1.0	5.8	19.0	9.2	8.6	12.7	5.3	2.2	cl
51	4.72–4.45	P2	2Bt2b1	35.7	26.9	37.4	2.2	2.2	4.9	17.5	9.0	9.5	11.7	5.6	14.0	cl
Soil Profile No. 85																
36	4.46–4.00	P3	2Btb2	25.4	22.7	51.9	1.0	1.1	2.9	12.3	8.1	7.1	10.3	5.3	2.2	c
37	4.00–3.71	P3	2BCtkb2	32.1	23.0	44.9	1.7	2.4	5.5	13.3	9.2	8.3	9.4	5.3	2.3	c
38	3.71–3.51	P4	3Atkb3	13.5	22.6	63.9	0.3	0.3	0.8	6.0	6.1	8.3	11.0	3.3	1.7	c
39	3.51–3.01	P4	3Btkb3	14.6	29.2	56.2	0.8	1.0	1.2	5.3	6.2	9.7	15.7	3.9	1.9	c
40	3.01–2.80	P4	3BCtk1b3	35.6	27.3	37.1	0.3	1.2	6.2	18.8	9.1	8.0	12.3	7.0	2.5	cl
41	2.80–2.59	P4	3BCtk2b3	42.0	25.5	32.5	1.3	3.0	7.6	19.6	10.5	8.6	11.7	5.2	7.0	cl
42	2.59–2.37	P4	4BCtb3	46.5	25.0	28.5	2.3	3.3	8.6	21.8	10.4	8.6	12.1	4.4	8.9	scl
43	2.37–2.25	P4	5BCtb3	54.7	18.8	26.5	6.7	6.0	8.4	21.9	11.7	6.4	8.7	3.7	70.2	gscl
Soil Profile No. 98																
128	1.58–1.20	P6	6Btb3	20.7	35.9	43.4	0.0	1.0	2.5	8.9	8.3	11.1	16.7	8.1	1.0	c-
Soil Profile No. 100																
59	5.37–4.87	P1	A	36.7	28.0	35.3	5.1	5.3	6.6	11.6	8.1	8.9	12.2	6.9	10.0	cl
61	4.77–4.10	P2	Abtb1	20.7	26.3	53.0	0.4	0.4	3.2	7.7	9.0	9.3	11.2	5.8	1.2	c
62	4.10–3.94	P3	Abtb2	18.2	25.6	56.2	0.4	0.2	1.3	8.0	8.3	12.2	11.9	1.5	1.2	c
63	3.94–3.66	P4	ABtkb2	19.0	29.6	51.4	0.3	0.5	2.0	6.6	9.6	11.8	11.4	6.4	1.2	c
64	3.66–3.27	P4	Btkb2	22.3	30.9	46.8	1.0	0.9	2.9	9.3	8.1	10.9	13.3	6.8	1.2	c
Soil Profile No. 125																
80	5.12–4.92	P1	A	32.9	32.2	34.9	5.6	6.0	6.0	8.8	6.5	9.6	14.2	8.4	16.8	gcl
81	4.92–4.69	P1	Bt1	29.6	31.0	39.4	5.2	6.1	5.4	6.8	6.2	8.2	12.6	10.1	11.2	cl+
82	4.69–4.27	P1	Bt2	31.9	30.8	37.3	5.1	5.7	6.9	8.4	5.8	9.0	12.5	9.3	12.0	cl
87	2.80–2.25	P5	3Btk1b2	22.3	35.7	42.0	0.9	0.8	1.2	8.8	10.5	12.2	16.4	7.2	2.5	c–
88	2.25–1.86	P5	3Btk2b2	23.0	34.4	42.6	0.5	0.5	0.4	9.6	12.0	15.0	15.0	4.4	0.0	c–
89	1.86–1.57	P5	4BCtb2	44.5	20.8	34.7	8.0	8.1	9.4	13.6	5.4	6.2	8.6	6.0	16.5	gcl–
90	1.57–1.42	P5	5BCtb2	52.9	16.4	30.7	11.8	11.5	14.0	10.7	4.9	4.4	7.1	4.9	63.5	gscl

Note: All samples from the northeast wall of 1989 trench (Fig. 2) unless otherwise noted. Trench elevations are given with respect to bottom of exposure. Lower case "b" followed by a number designates a buried paleosol horizon. Abbreviations and definitions are given in Soil Survey Staff (1951, 1975). Particle size classes in millimeters.

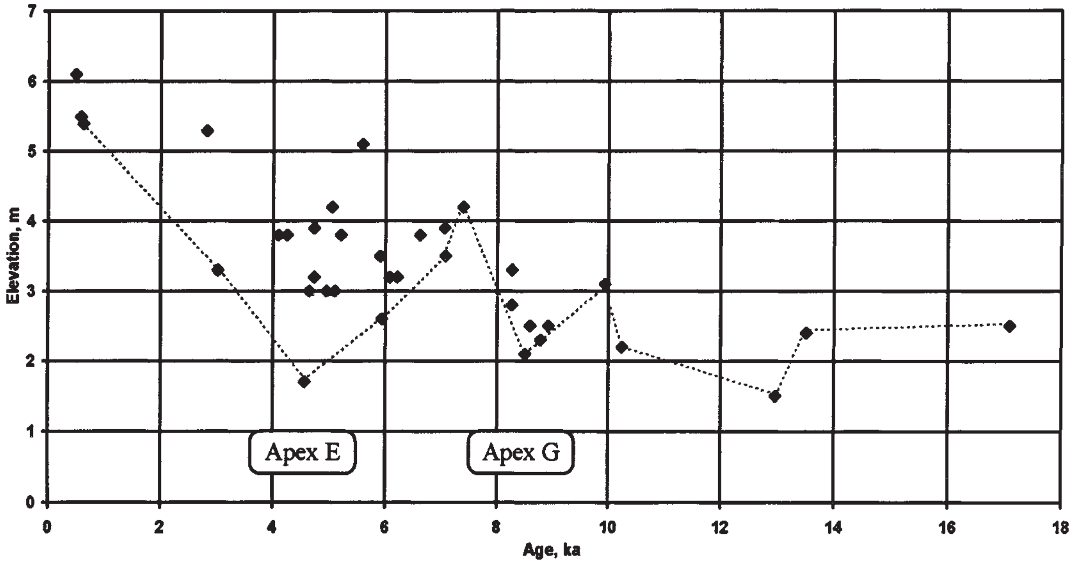

Figure 4. Charcoal ages as a function of trench elevation. Dotted line portrays the minimum elevations for which we have direct age control.

from thinly bedded sediment at the base of channel C3.3 (Fig. 3B, station 74). Thinly bedded sediments in the small channel at the northwest end of channel C4.1 were undisturbed by pedoturbation, indicating that they were quickly buried after 8.3 ka. Paleosol P3 probably covered the entire surface of the fan, but was severely eroded between station 0 and station 80. The best-developed section is soil profile 85 (Table 2; Fig. 3B).

Paleosol P4. This paleosol has a 20-cm-thick, very dark grayish-brown Atk horizon with strong angular blocky structure overlying a 50-cm-thick, dark grayish-brown Btk horizon with prismatic structure (Table 3, soil profile 85; Fig. 6). The brown clay loam BCtk horizon overlies a 100-cm-thick, carbonate-free section containing five dark yellowish-brown BCt horizons with textures ranging from clay loam to gravel. Both the A and B horizons have a pH higher than 8, and both have vertically oriented calcite filaments and fine nodules (denoted Bk2 in Fig. 3). Where early aggradation was especially rapid, the nodules are underlain by a horizon containing only calcite filaments (denoted Bk3 in Fig. 3). Both the clay films and the carbonate in the Atk horizon formed after its burial by the overbank deposit associated with paleosol P3. The nodules in the Bk2 are at ped intersections and sometimes are cavernous (Fig. 7). The t_o for this paleosol is about 10 ka. A charcoal sample dated as 10.2 ka was in a channel fill that appeared to be contemporaneous with a Bk3 remnant near station 68 (Fig. 3A). The youngest date in the underlying paleosol was 9.9 ka at station 139 (Table 1; Fig. 3B). Paleosol P4 was once the surface soil throughout the trench, but it was severely eroded between station 45 and station 80.

Paleosol P5. This paleosol has a 45-cm-thick, dark brown Bt horizon with medium strong prismatic structure overlying a 100-cm-thick, dark brown CBt horizon (Fig. 6). Although the texture of the Bt horizon is clay, the texture of the CBt horizon is gravel to sandy clay and the structure is loose (Table 3, soil profile 103). Both horizons have a pH less than 7.5, contain no calcite, and have common to many medium thick clay films lining pores and coating clasts. There is a remnant of paleosol P5 at station 67 (Fig. 3A) and a continuous section exists between station 101 and 150, where its relatively level surface shows no sign of erosion having removed a former A horizon (Fig. 3B). The B horizon characteristics in the surface of this paleosol presumably were imprinted during the early pedogenesis of paleosol P4. Paleosol P5 began forming before 17.1 ka (Fig. 3B, station 120).

Paleosol P6. This paleosol has a 36-cm-thick, dark brown Bt horizon with a coarse strong subangular structure (Table 3, soil profile 98; Fig. 6). Many medium thick clay films line pores, and a few thin clay films coat clasts. Although the pH is 8.0, no calcite is present. Fossils of Pleistocene fauna (camel and horse teeth) overlie paleosol P6 between stations 89 and 94 (Fig. 3B). A slightly eroded section of paleosol P6 exists between stations 87 and 150. Paleosol P6 began forming before 17.1 ka (Fig. 3B, station 120). We estimate its t_o at about 24 ka, because it has characteristics almost identical to paleosol P5, which had a t_d of about 7 ka.

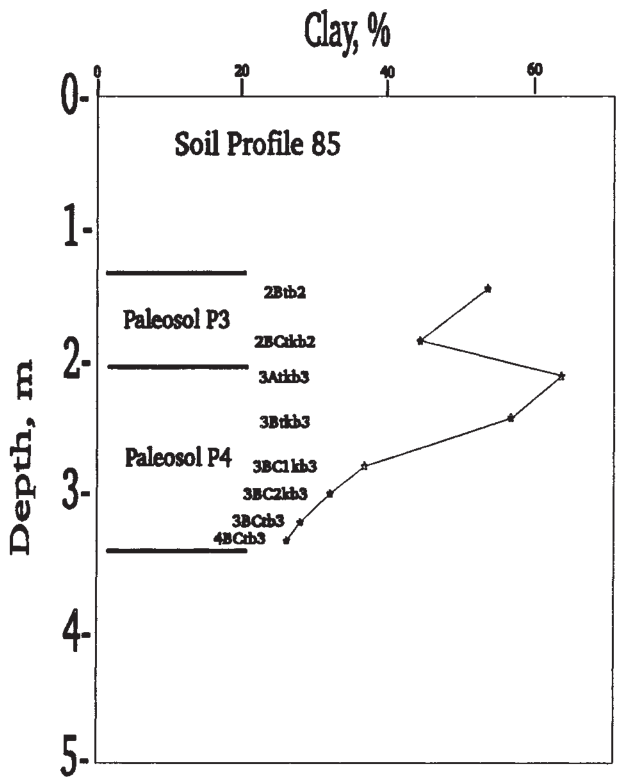

Figure 5. Clay concentration as a function of depth in soil profile 85. The interruption in upward fining occurred at 8.3 ka, when abandonment of a fault offset in the stream (Lienkaemper and Borchardt, 1996) shortened the flow path, bringing slightly coarser overbank deposits to the site.

TABLE 4. PEDOCHRONOLOGY OF THE DOMINANT PALEOSOLS IN THE MASONIC CREEK ALLUVIAL FAN AND AGES OF THE CHANNELS THAT CUT THEM OR CONTRIBUTED TO THEIR DEPOSITION

Paleosol	t_o*	t_b	t_d	Calcite	Channels	Dates in channels
Modern	0.5	0.0	0.5	No	Masonic	Modern
P1	4.6	0.5	4.1	No	C1	0.5, 0.6, 0.6, 2.8, 4.1, 5.6†, 6.1†
P2	7.1	4.6	2.5	No	C2	3.0†, 4.3†, 4.6, 4.6, 4.7, 4.7, 5.0, 5.1, 5.1, 5.2, 5.9, 5.9, 6.2, 6.2, 6.6
P3	8.3	7.1	1.2	Yes	C3	7.1, 7.1, 7.4
P4	10.0	8.3	1.7	Yes	C4	8.3, 8.3, 8.5, 8.6, 8.9, 10.2
P5	>17.1	10.0	~7.0	No	C5	9.9†, 13.0, 13.5
P6	~24.0	>17.1	~7.0	No	C6	17.1

Note: *t_o—age when soil formation or aggradation began, ka; t_b—age when soil or strata was buried, ka; t_d—duration of soil development or aggradation, k.y.

†Discordant date.

DISCUSSION

This discussion proposes a source for the calcite, describes the nature of the soil environment in which it formed, and asserts its possible significance for climatic history in the Bay Area.

Source of the Calcite

The formation of calcite in soils developed on noncalcareous parent materials is normally considered an arid to semiarid environmental phenomenon. The source of the calcium and of the carbonate at Union City is of primary concern. Desert soils can accumulate huge amounts of calcite (to 90% or more) simply by incorporating calcareous dust blown from limestone outcrops (Gardner, 1972; McFadden and Tinsley, 1985; McFadden et al., 1991). However, at Union City, the prevailing winds cross no known sources of surficial carbonate. Carbonate rocks were not observed in the alluvium or in the alluvial source area. There has been no significant change in the source of the sediments before, during, and after the period of calcite precipitation.

Although highly visible in paleosols P3 and P4, calcite is only 0.15% of the soil (Table 5). Trace amounts such as these do not require a mineralogical source for the carbonate. Soils commonly derive CO_2 through root respiration and plant decay, which is a function of vegetative ground cover (Quade and Cerling, 1990; Amundson et al., 1989). In young alluvial sediments like those deposited at the site, the source of immediately and readily available calcium is the exchange complex of the associated 2:1 layer silicates. Thus, a relatively unweathered Miocene shale from the East Bay Hills was found to have 23.5 $cmol_c$ (centimole charge) of extractable Ca per kg of material (Borchardt, 1984). This is enough to yield 11.8 g $CaCO_3$/kg of soil during normal acidification with CO_2-laden rainwater. A 40-cm-thick soil column would yield about 1 g $CaCO_3/cm^2$. The young, clayey alluvial soils at our site had a total of only 0.51 g $CaCO_3/cm^2$ in the soil column (Table 5)—well within expectations for in situ formation of the calcite. Note also that this is a pedogenic calcite accumulation rate of 0.17 g/cm^2/k.y., similar to the rule of thumb (0.20 g/cm^2/k.y.) suggested by Birkeland (1984) for soils in general.

Calcite from paleosols P3 and P4, which formed between 10 and 7 ka, had Holocene ages concordant with pedogenic formation (Table 5). Calcite from ground water or from limestone might have been much older. The measured ages were slightly less than the theoretical ages calculated from the dates for the associated charcoal. This is probably due to the tendency for dissolution and reprecipitation to continue long after the initially fine crystals of calcite have formed. The cavernous nodules that formed at ped intersections are evidence for reprecipitation (Fig. 7). Reprecipitation occurs in the presence of carbonic acid derived from new respiration and decay of plants in the overlying soil. Each cycle combines a mole of fresh CO_2 with each mole of CO_3^{2-}, diluting the old carbon with the new. Thus, as might be expected, the upper horizon is more affected than the lower one (Table 5). In addition, the $\delta^{13}C$ values of the samples were typical for pedogenic calcite formed via root respiration and decay of plants using the C_3

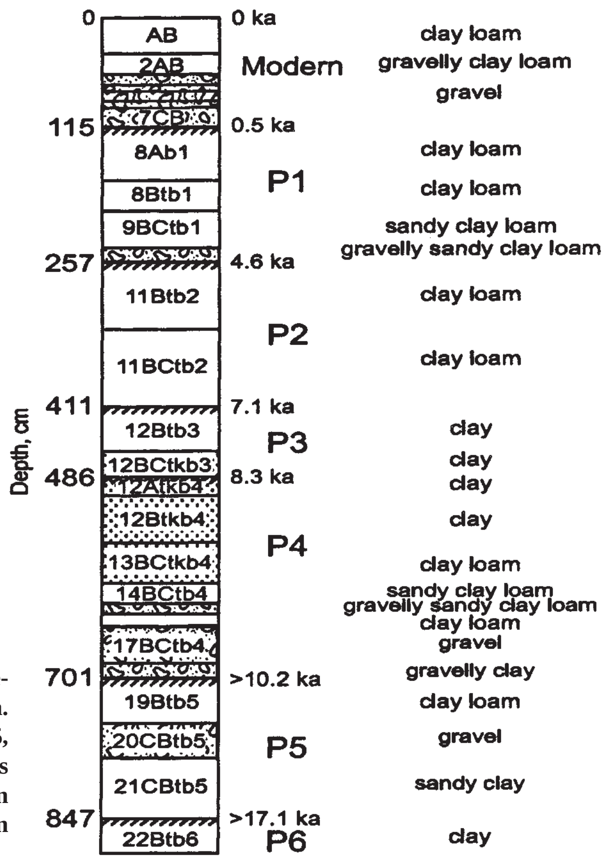

Figure 6. Composite soil profile from measurements of the oldest (t_d) representatives of the soils developed on the alluvial fan at Union City, California. The data were from portions of the best-developed sections in soil profiles 25, 67, 85, 103, and 98. Hachures represent former surfaces of the paleosols (P1–P6). Dot pattern and k designation indicate pedogenic calcite. Soil horizon designations prefixed with Arabic numerals indicating 22 significant changes in parent material (t—evidence for clay films; b—buried soil).

TABLE 5. ^{14}C AGES AND STABLE ISOTOPE DATA OF CALCITE INITIALLY PRECIPITATED BETWEEN 10 KA AND 7 KA IN SOIL PROFILE 81

Sample number	Beta lab number	Paleosol	Calcite (g/100 g)	Thickness (cm)	Bulk density* (g/cm^3)	Total calcite† (g)	Theoretical age§ (ka)	Measured age (ka)	Difference (k.y.)	$\delta^{13}C$ (‰)
89B351	113914	P3	0.14	60	2.20	0.19	7.7	4.3	3.3	–12.5
89B352	113915	P4	0.15	105	2.01	0.32	9.2	7.6	1.6	–12.3

Note: Calcite content, measured ^{14}C age of calcite (standard deviation = 0.1 k.y.), and $\delta^{13}C$ were determined by Beta Analytic, Inc., Miami, Florida.
*Measured by Soil Mechanics Laboratory, Oakland, California, on soil clods from equivalent samples 89B037 and 89B040 from Soil Profile 85.
†Total calcite in a cm^2 soil column = area, cm^2 × calcite, g/100 g × soil thickness, cm × bulk density, g/cm^3.
§Theoretical age = $t_b + (t_o - t_b)/2$, where t_b and t_o for the Bk1 were 7.1 and 8.3 ka. The t_o for the Bk2 was assumed to be 10 ka.

(temperate zone) photosynthetic pathway common to the site (Cerling et al., 1989). Although probably not expected, even during the early Holocene dry period, C_4 (arid zone) plants were not significant at the site and there is no trace of the influence of marine carbonate contamination. Either of these possibilities would have yielded $\delta^{13}C$ values near zero.

Nature of the Soil Environment

The thickest Bk horizons in this exposure are preserved where thick overbank deposits associated with paleosols P3 and P4 are overlain by thick overbank deposits associated with paleosols P1 and P2 (Fig. 3B, soil profile 85). In this alluvial fan, coarse channel fill material generally does not collect calcite (Fig. 3B, soil profile 75). To the northwest of station 85 the Bk horizon diminishes in thickness, eventually becoming uniformly 10 cm thick (Fig. 3B, stations 103 to 120). Thus, the 140-cm-thick Bk horizon in soil profile 85 seems to have formed in response to increasing aggradation that influenced stations southeast of soil profile 103 (Fig. 3B). Calcite precipitation was spread throughout an increasingly wide zone as the elevation of the wetting front was raised with each additional increment of alluvium. Except for the hiatus that occurred at the P3-P4 paleosol boundary (Fig. 5), alluvial deposition must have been relatively continuous. Horizons containing calcite filaments exist above and below those containing fine nodules in soil profile 85 (Fig. 3B; Table 2). Only nodules exist in soil profile 103 (Fig. 3B) and farther northwest, where the alluvial cover is thin. The “refugia” hypothesis provides an explanation.

Calcite filaments are the first to form in soils, whereas the nodules appear to develop as refugia following extraordinarily wet years. Being thin and delicate, the smallest filaments would be the first to dissolve during those years when carbonic-acid–laden rainwater percolates beyond the normal wetting front. When the soil finally dries out and solution concentrations increase, calcite precipitates where the soil pH is highest; i.e., adjacent to the thickest filaments that escaped dissolution. Repetitions of this cycle no doubt produce increasingly thick filaments, calcans (calcitic ped coatings), and cavernous nodules at ped junctions (Fig. 7). With still more repetitions of the cycle, solid nodules develop. In another study, nodules dated as 26 ka were equidimensional (5 cm diameters) and equidistant (on 10 cm centers) (Borchardt and Seelig, 1991). The conditions for calcite formation change from season to season, year to year, and from place to place. Refugia (nodules) are favorable places for calcite precipitation and moderately unfavorable places for calcite dissolution.

The filaments at the base of the Bk probably indicate that rapid aggradation occurred during the early life of paleosol P4 at station 85, and the overlying zone of nodules indicates a later period of relative stability. The profile at station 103, however, lacked early aggradation and subsequently tended to incorporate the relatively thin alluvial deposits that produced a distinct P3 paleosol elsewhere.

With time, illuviation normally produces a “clay bulge,” wherein the A horizon of a soil loses clay to the B horizon immediately beneath it. The lack of such a bulge in paleosol P4 is concordant with its short development time. A plot of clay concentration as a function of depth in soil profile 85, however, shows more clay in the 3Atkb3 horizon than in the underlying horizons (Fig. 5). This type of depth function is typical for alluvial units that were subject to upward fining, a common characteristic of overbank depo-

Figure 7. Pedogenic calcite filaments and nodules that formed between 10 ka and 7 ka (Fig. 3B, station 81). In the early stage of development some of the filaments form as pore linings and others form along ped faces, generally as dendritic forms. In the later stage of development cavernous nodules form by coating blocky peds at their intersections.

sition (Davis, 1983). Soil development must be superimposed on such materials. Under similar conditions 6 km to the southeast, we found that the imprint produced by upward fining remains for at least 2.4 k.y. after the last depositional event (Borchardt et al., 1988). Both P3 (t_d = 1.2 ka) and P4 (t_d = 1.7 ka) show the imprint of upward fining and the lack of evidence for illuviation (except for a few clay films).

The upward fining characteristic of the parent material for paleosol P4 was interrupted when the parent material for paleosol P3 began to bury it during a new phase of upward fining (Fig. 5). This occurred at 8.3 ka, when the fan apex apparently shifted about 25 m to the southeast due to accumulated offset along the Hayward fault (Lienkaemper and Borchardt, 1996).

We reiterate that, at this trench site, the modern soil, as well as paleosols P1 and P2, all formed since 7.1 ka and have no signs of pedogenic calcite (Fig. 3). All calcitic horizons at the site are at least 1 m below surfaces younger than 7.1 ka. Older surfaces in this ecotome may have formed pedogenic calcite in the past, but it would have been dissolved and leached away like the exchangeable sodium in an Alberta paleosol described by Sanborn and Pawluk (1980). That paleosol initially developed as a sodic soil between 13 ka and 7 ka. It now has many of the properties of a modern sodic soil, but lacks the sodium. The removal of the sodium probably was the result of an increase in precipitation after 7 ka.

Estimating Mean Annual Precipitation During Early Holocene Time

Paleosols, being fossil soils, often provide a record of past climates (Retallack, 1981, 1983; Birkeland, 1984). To record evidence for mean annual precipitation during the early Holocene dry period, calcareous paleosol P3 would have to be buried immediately thereafter. At our site, a hypothesized increase in rainfall apparently terminated calcite formation while leading to its preservation via accelerated aggradation. The tiny, 20-cm-deep channel C3.2 at station 79 was active until 7.1 ka, when it apparently was abandoned for the more direct, slightly deeper channel C3.1 at station 68 (Fig. 3, A and B). As rainfall increased over the next 2.5 k.y., the stream made major cuts in the P3 surface at three different places in the trench (Fig. 3A; stations 63, 24, and 38). The associated overbank deposition quickly buried paleosol P3 by the unit that was to form paleosol P2 during the next 2.5 k.y. This burial, by a clay loam overbank deposit now ranging in thickness from 52 to 78 cm (Table 6), helped to protect the calcite in paleosol P3 from subsequent dissolution.

Leaching Depth During the Dry Period. Three P3 paleosol remnants buried at 7.1 ka have level surfaces with horizontal extents showing that they were not eroded before burial (Fig. 3, stations 34, 71, and 85; Table 6). Each of the upper portions of these paleosol remnants contains a B horizon in which calcite is absent. The top of this B horizon probably was once an A horizon that attained some B horizon properties (e.g., a few thin clay films) after burial. The thickness of this noncalcareous horizon provides a record of the leaching depth when the soil was at the surface, assuming that no calcite was added to it or subtracted from it after burial. The buried, noncalcareous, uneroded horizon at the top of paleosol P3 has an average thickness of only 41 ± 3 cm (Table 6). This appears to have been the leaching depth shortly before the rapid burial of paleosol P3 at 7.1 ka. We estimate that at least 30 cm of overbank material would have been required to protect channel C3.2 from pedoturbation (Fig. 3B).

Leaching Depth at the Present Time. At this site, the leaching depth under the present climate is less than 100 cm. This is shown by the thickness of the noncalcareous horizon beneath the modern undifferentiated fill and colluvium between stations 95 and 120 (Fig. 3B). Here, on the flank of the alluvial fan, only a thin remnant of the Bk horizon remains out of reach of present effective rainfall. Only a few nodules remain in the horizon; the calcite filaments probably were dissolved before burial was sufficient to preserve them. Some of this leached calcite was trapped throughout the underlying clayey Bt horizon of Pleistocene paleosol P5 (Table 3, soil profile 125). Still farther from the fan axis, where the burying material is less than 100 cm thick, there is no Bk horizon.

Elsewhere in western Alameda County slightly drier sites (mean annual precipitation <400 mm/yr) have modern calcitic soils that are leached to depths between 70 and 130 cm (Welch, 1981). Even at mean annual precipitations of 470 mm/yr, soils with restricted drainage still accumulate calcite. A clay loam soil under slightly restricted drainage 6 km to the southeast had a leaching depth of 70 cm (Borchardt et al., 1988). Thus, the current leaching depth at Masonic Creek now appears to be between 70 and 100 cm.

According to the classical relationship devised for California and Nevada soils by Arkley (1963), a 41 cm leaching depth in clay loam would reflect a mean annual precipitation of about 260 mm/yr, while a 75 cm leaching depth would be expected for today's mean annual precipitation of 470 mm/yr. In the unlikely event that early Holocene rainfall occurred in the summer as well as the winter, leaching depths could decrease without a decrease in mean annual precipitation (McFadden and Tinsley, 1985). However, there is no evidence that seasonality of precipitation and evapotranspiration was significantly different at our site during early Holocene time (COHMAP, 1988). Further analysis along this line is not warranted because of the limitations of the data from our site. For an accurate determination of mean annual precipitation during early Holocene time, we would have to discover and study additional sites and consider the water-holding capacities of the soils along with numerous other factors. Nevertheless, the fact remains that the leaching depths for these early Holocene paleosols are about half of those for modern soils in the area. We infer that precipitation during early Holocene time was about half of the current level.

Initiation of the Dry Period

Overbank deposition associated with paleosol P4 began between 9.9 and 10.2 ka (Fig. 3B, station 139, and Fig. 3A, station 68; Table 4). No pedogenic calcite appears to have formed during the early part of this deposi-

TABLE 6. THICKNESS OF NONCALCAREOUS ZONE IN PALEOSOL P3 REMNANTS BURIED BY CLAY LOAM PALEOSOL P2 AT 7.1 KA AND HAVING LATERAL EXTENTS OF MORE THAN 1 M

Soil profile number	Noncalcareous horizon	Texture	Depth to Bk in P3 (cm)	Depth of P2 burial (cm)	Lateral extent of section (m)
34	3Bb3	cl*	38	78	1
71	5Btb2	l	38	52†	3
85	2Btb2	c	46	57	11
Average			41 ± 3		

Note: *c—clay, l—loam.
†Depth measurement excludes highly permeable 15 cm cobble horizon at base of P2.

tional phase, as indicated by the noncalcareous Bt horizon that underlies the Bk horizon in soil profile 103 (Fig. 3B). This Bt horizon has some medium thick clay films, while the Btk above it has thin clay films. Thus, during the early development of paleosol P4, annual percolation must have reached this horizon, carrying a significant amount of suspended clay. With accelerated aggradation and restriction of the wetting front to the top of the Btk horizon, clay film deposition ceased at this depth.

The regional picture likewise shows that a dramatic change in climate occurred at about 10 ka. Certain sensitive sites demonstrate the overall pattern. For example, in northeastern California, Honey Lake all but dried up at the end of Pleistocene time (Wills and Borchardt, 1993). Water tables dropped in formerly wet meadows in Yosemite National Park, allowing forests to invade at 9.9 ka (Wood, 1984). Similarly, a dry postglacial climate beginning at 10.3 ka apparently caused a vegetative die-off and extensive colluviation in the nearby Sierran foothills (Borchardt et al., 1980). The Union City locality simply reflected a significant meteorological change that was occurring throughout California.

Termination of the Dry Period

The termination of the dry period at the study site seems to have occurred after 7.1 ka. Between 8.3 ka and 7.1 ka Masonic Creek drained through a series of nested channels in the area marked by stations 72 to 80 (Fig. 3B). The youngest of these was only 20 cm deep (Fig. 3B, station 79) when it was abandoned for a slightly deeper channel to the southeast (Fig. 3A). The progression must have been rapid, because charcoal in the channel at station 79 and charcoal in the transition material at station 69 have the same date, 7.1 ka. By 5.9 ka the base level seems to have dropped more than 2 m (Fig. 3A, station 63; Fig. 4). Perhaps the hypothesized increase in rainfall was responsible for the drop in base level.

It is possible that the cessation of pedogenic calcite formation is related only to local changes in microclimate. The depositional curves of Atwater et al. (1977), for example, show that the width of San Francisco Bay at the latitude of the study site increased from 2 km to 10 km after 7 ka. This brought the shoreline to within 10 km of the study site. This large expanse of water undoubtedly would have moderated the local climate at Masonic Creek's sensitive ecotome by gradually producing cooler summers and warmer winters.

Nevertheless, the change from dry to wet at the end of early Holocene time remains pivotal in Holocene paleoclimatic studies in many other ecologically sensitive areas. Several studies show that the end of the worldwide Altithermal varied depending on the location and relation to the jet stream. In the state of Washington, for example, pollen from lake sediments show that the early Holocene dry period lasted until 7 ka in the western part of the state and until 5 ka in the eastern part (Baker, 1983). In Utah, a warm interval occurred from 7 to 4 ka (Baker, 1983). In Wisconsin, the prairie invasion from the west reached its maximum at 7 ka and the oak (*Quercus*) invasion from the south reached its maximum at 6 ka. After this, the prairie retreated entirely from the state and oak retreated to the southern half (Webb et al., 1983). A warm and dry period occurred in the eastern states, ending between 4 and 6 ka (Bierman et al., 1997). Evidence from pack rat (*Neotoma*) middens show that the southwestern deserts were relatively cool until 8 ka (Van Devender, 1977), when the storm track presumably shifted to the north. Thus, the climatic effect of the Altithermal varies from place to place due to the complex interactions of global and local weather patterns.

Prehistoric vegetative data for the Union City area are nonexistent, and those for California are limited to specific regions. Until recently, only a few pollen sites in the state had been studied: Osgood Swamp in the eastern Sierra Nevada (Adam, 1967), Santa Barbara Channel (Heusser, 1978), and Clear Lake (Adam, 1988). These particular sites show the major shifts between glacial and interglacial climates, but appear to be insensitive to minor changes during the Holocene. This is perhaps because they sample large areas or are not at appropriately sensitive ecotomes like the one at our site. Only those locations that have a mean annual precipitation near 500 mm/yr would show the effect.

The nearest sensitive site appears to be in the southern Sierra Nevada, where pollen studies show that after 6.5 ka, open pine and oak forests were displaced by mountain hemlock, red fir, and giant sequoia (Anderson and Smith, 1994). Elsewhere in California, pluvial lakes that had been dry since the end of Pleistocene time began refilling after 7 ka (Batchelder, 1970; Smith, 1979; Wills and Borchardt, 1993). Because the prevailing winds are westerly, the paleoclimate of the Sierra Nevada no doubt reflects the paleoclimate of the San Francisco Bay area. According to Reneau et al. (1990), aggradation in hillslope hollows in the San Francisco Bay area was dominant during the dry period, eventually yielding to debris-flow activity after 7 ka.

CONCLUSIONS

1. Pedogenic carbonate formed at Union City, California, in early Holocene time between 10 and 7 ka.
2. Little, if any, pedogenic carbonate formed at Union City after 7 ka.
3. Leaching depths during the early Holocene dry period may have been about half the current depths. Thus, we estimate that precipitation during that time may have been as little as half of today's 470 mm/yr.
4. Evidence for this dry period will be found only in soils that underwent rapid aggradation at the end of the dry period at 7 ka.

ACKNOWLEDGMENTS

Research was supported in part by the California Division of Mines and Geology and the U.S. Geological Survey (USGS), Department of the Interior, under USGS award numbers 14-08-0001-21929 and 14-08-0001-G2078. We thank Masonic Homes, Union City, for their kind cooperation and for permission to excavate on their property, Jim McFarlane of the CALTRANS Soil Testing Laboratory, who conducted the particle-size analyses, Tim Jull of the National Science Foundation–National Accelerator Facility for Radioisotope Analyses for determining the ^{14}C dates for charcoal samples by using the accelerator mass spectrograph, and Jim Buckley of Teledyne Isotopes, Inc., for determining the age of sample 89B031 via conventional ^{14}C analysis. We also thank Ron Amundson, Bill Bryant, Jerry Treiman, Leland Gile, Jennifer Harden, Katherine Kendrick, James West, Les McFadden, and John Ritter, who kindly reviewed early versions of the manuscript.

The views and conclusions contained in this document are those of the authors and should not be interpreted as necessarily representing the official policies, either expressed or implied, of the state of California or of the U.S. Government.

REFERENCES CITED

Adam, D. P., 1967, Late-Pleistocene and Recent palynology in the central Sierra Nevada, *in* Cushing, E. J., and Wright, H. E., Jr., eds., Quaternary paleoecology (INQUA Congress VII, Proceedings 7): New Haven, Connecticut, Yale University Press, p. 275–301.

Adam, D. P., 1988, Palynology of two upper Quaternary cores from Clear Lake, Lake County, California: U.S. Geological Survey Professional Paper 1363, 86 p.

Amundson, R. G., Chadwick, O. A., Sowers, J. M., and Doner, H. E., 1989, The stable isotope chemistry of pedogenic carbonates at Kyle Canyon, Nevada: Soil Science Society of America Journal, v. 53, p. 201–210.

Anderson, R. S., and Smith, S. J., 1994, Paleoclimatic interpretations of meadow sediment and pollen stratigraphies from California: Geology, v. 22, p. 723–726.

Arkley, R. J., 1963, Calculation of carbonate and water movement in soil from climate data: Soil Science, v. 96, p. 239–248.

Atwater, B. F., Hedel, C. W., and Helley, E. J., 1977, Late Quaternary depositional history, Holocene sea-level changes, and vertical crustal movement, southern San Francisco Bay, California: U.S. Geological Survey Professional Paper 1014, 15 p.

Baker, R. G., 1983, Holocene vegetational history of the western United States, *in* Wright, H. E., Jr., ed., Late-Quaternary environments of the United States: Volume 2. The Holocene: Minneapolis, University of Minnesota Press, p. 109–127.

Bard, E., Hamelin, B., Fairbanks, R. G., and Zindler, A., 1990, Calibration of the ^{14}C timescale over the past 30,000 years using mass spectrometric U-Th ages from Barbados corals: Nature, v. 345, p. 405–410.

Batchelder, G. L., 1970, Post-glacial ecology at Black Lake, Mono County, California [Ph.D. thesis]: Tucson, Arizona State University, 180 p.

Bierman, P., Lini, A., Zehfuss, P., Church, A., Davis, P. T., Southon, J., and Baldwin, L., 1997, Postglacial ponds and alluvial fans: Recorders of Holocene landscape history: GSA Today, v. 7, no. 10, p. 1–9.

Birkeland, P. W., 1984, Soils and geomorphology: New York, Oxford University Press, 372 p.

Borchardt, G., 1984, Stabilization of landslides: Effects of various chemicals on the laboratory shear strength of an expansive soil: California Division of Mines and Geology Special Report 155, 65 p.

Borchardt, G., 1992a, Holocene slip rate of the Hayward fault, Union City, California: U.S. Geological Survey National Earthquake Hazards Reduction Program Final Technical Report, 58 p.

Borchardt, G., 1992b, Pedochronology along the Hayward fault, *in* Borchardt, G., Hirschfeld, S. E., Lienkaemper, J. J., McClellan, P., Williams, P. L., and Wong, I. G., eds., Proceedings of the Second Conference on Earthquake Hazards in the Eastern San Francisco Bay Area: California Department of Conservation, Division of Mines and Geology Special Publication 113, p. 111–117.

Borchardt, G., and Seelig, K. A., 1991, Soils, paleosols, and Quaternary sediments offset along the Hayward fault at Point Pinole regional shoreline, Richmond, California, *in* Sloan, D., and Wagner, D. L., eds., Geologic excursions in northern California: San Francisco to the Sierra Nevada: California Department of Conservation, Division of Mines and Geology Special Publication 109, p. 75-83.

Borchardt, G., Rice, S., and Taylor, G., 1980, Paleosols overlying the Foothills fault system near Auburn, California: California Division of Mines and Geology Special Report 149, 38 p.

Borchardt, G., Lienkaemper, J. J., and Schwartz, D. P., 1988, Soil development and tectoturbation in a toposequence produced by Holocene downwarping along the Hayward fault, Fremont, California, *in* Borchardt, G., ed., Soil development and displacement along the Hayward fault (Volume I): Fremont, California Division of Mines and Geology Open-File Report DMG OFR 88-12, p. 53-112.

Cerling, T. E., Quade, J., Wang, Y., and Bowman, J. R., 1989, Carbon isotopes in soils and palaeosols as ecology and palaeoecology indicators: Nature, v. 341, p. 138–139.

COHMAP Members, 1988, Climatic changes in the last 18,000 years: Observations and model simulations: Science, v. 241, p. 1043–1052.

Colman, S. M., Pierce, K. L., and Birkeland, P. W., 1987, Suggested terminology for Quaternary dating methods: Quaternary Research, v. 28, p. 314–319.

Davis, R. A., Jr., 1983, Depositional systems: A genetic approach to sedimentary geology: Englewood Cliffs, New Jersey, Prentice-Hall, 669 p.

Gardner, L. R., 1972, Origin of the Morman Mesa caliche, Clark County, Nevada: Geological Society of America Bulletin, v. 83, p. 143–156.

Gile, L. H., Peterson, F. F., and Grossman, R. B., 1966, Morphological and genetic sequences of carbonate accumulation in desert soils: Soil Science, v. 101, p. 347–360.

Heusser, L., 1978, Pollen in Santa Barbara basin, California: A 12,000-year record: Geological Society of America Bulletin, v. 89, p. 673–678.

Lienkaemper, J. J., and Borchardt, G., 1996, Holocene slip rate of the Hayward fault at Union City, California: Journal of Geophysical Research, v. 101, no. B3, p. 6099–6108.

Linick, T. W., Long, A., Damon, P. E., and Ferguson, C. W., 1986, High-precision radiocarbon dating of bristlecone pine from 6554 to 5350 B.C: Radiocarbon, v. 28, p. 943–953.

McFadden, L. D., and Tinsley, J. C., 1985, Rate and depth of pedogenic-carbonate accumulation in soils: Formulation and testing of a compartment model, *in* Weide, D. L., and Faber, M. L., eds., Soils and Quaternary geology of the southwestern United States: Geological Society of America Special Paper 203, p. 23–41.

McFadden, L. D., Amundson, R. G., and Chadwick, O. A., 1991, Numerical modeling, chemical, and isotopic studies of carbonate accumulation in soils of arid regions, *in* Nettleton, N. D., ed., Occurrence, characteristics, and genesis of carbonate, gypsum, and silica accumulations in soils: Soil Science Society of America Special Publication 26, p. 17–35.

Quade, J., and Cerling, T. E., 1990, Stable isotopic evidence for a pedogenic origin of carbonates in Trench 14 near Yucca Mountain, Nevada: Science, v. 250, p. 1549–1552.

Rantz, S. E., 1971, Mean annual precipitation and precipitation depth-duration-frequency data for the San Francisco Bay region, California: U.S. Geological Survey, San Francisco Bay Region Environment and Resources Planning Study Basic Data Contribution 32, 5 p., 1 plate, scale 1:250,000.

Reneau, S. L., Dietrich, W. E., Donahue, D. J., Jull, A. J. T., and Rubin, M., 1990, Late Quaternary history of colluvial deposition and erosion in hollows, central California Coast Ranges: Geological Society of America Bulletin, v. 102, p. 969–982.

Retallack, G., 1981, Fossil soils: Indicators of ancient terrestrial environments, *in* Niklas, K. J., ed., Paleobotany, paleoecology and evolution (Volume 1): New York, Praeger, p. 55–102.

Retallack, G. J., 1983, Late Eocene and Oligocene paleosols from Badlands National Park, South Dakota: Geological Society of America Special Paper 193, 82 p.

Sanborn, P., and Pawluk, S., 1980, An early Holocene Solodic paleosol near Priddis, Alberta: Canadian Journal of Earth Sciences, v. 17, p. 1323–1330.

Smith, G. I., 1979, Subsurface stratigraphy and geochemistry of late Quaternary evaporites, Searles Lake, California: U.S. Geological Survey Professional Paper 1043, 130 p.

Soil Survey Staff, 1951, Soil survey manual: USDA-SCS Agriculture Handbook 18: Washington, D.C., U.S. Government Printing Office, 503 p.

Soil Survey Staff, 1975, Soil taxonomy: A basic system of soil classification for making and interpreting soil surveys: USDA-SCS Agriculture Handbook 436: Washington, D.C., U.S. Government Printing Office, 754 p.

Stuiver, M., and Reimer, P. J., 1993, Extended ^{14}C database and revised CALIB radiocarbon calibration program: Radiocarbon, v. 35, p. 215–230.

Stuiver, M., Braziunas, T. F., Becker, B., and Kromer, B., 1991, Climatic, solar, oceanic and geomagnetic influences of Late-Glacial and Holocene atmosphere $^{14}C/^{13}C$ change: Quaternary Research, v. 35, p. 1–24.

Van Devender, T. R., 1977, Holocene woodlands in the southwestern deserts: Science, v. 198, p. 189–192.

Webb, T., III., Cushing E. J., and Wright, H. E., Jr., 1983, Holocene changes in the vegetation of the Midwest, *in* Wright, H. E., Jr., ed., Late-Quaternary environments of the United States: Volume 2. The Holocene: Minneapolis, University of Minnesota Press, p. 142–165.

Welch, L. E., 1981, Soil survey of Alameda County, California, western part: U.S. Department of Agriculture, Soil Conservation Service, in cooperation with University of California Agriculture Experiment Station, 103 p.

Wills, C. J., and Borchardt, G., 1993, Holocene slip rate and earthquake recurrence on the Honey Lake fault zone, northeastern California: Geology, v. 21, p. 853–856.

Wood, S. H., 1984, East Meadow of Aspen Valley, western Yosemite National Park, *in* Stine, S., Wood, S., Sieh, K., and Miller, C. D., eds., Holocene paleoclimatology and tephrochronology east and west of the central Sierran crest (Field Trip Guidebook of the Friends of the Pleistocene, Pacific Cell, October 12–14): Friends of the Pleistocene, p. 1–20.

MANUSCRIPT RECEIVED BY THE SOCIETY MARCH 6, 1997
REVISED MANUSCRIPT RECEIVED MAY 28, 1998
MANUSCRIPT ACCEPTED AUGUST 28, 1998

Printed in U.S.A.